EPJ Plus

EPJ.org
your physics journal

Eur. Phys. J. Plus (2019) **134**: 453 DOI 10.1140/epjp/i2019-12875-7

Correlation $\overline{\nu_p} - \sigma$ for U-Pu in the thermal and resonance neutron range via integral information

D. Rochman, A. Vasiliev, H. Ferroukhi, S. Pelloni, E. Bauge and A. Koning

Società Italiana di Fisica

Springer

Eur. Phys. J. Plus (2019) **134**: 453
DOI 10.1140/epjp/i2019-12875-7

THE EUROPEAN PHYSICAL JOURNAL PLUS

Regular Article

Correlation $\overline{\nu_p} - \sigma$ for U-Pu in the thermal and resonance neutron range via integral information

D. Rochman[1,a], A. Vasiliev[1], H. Ferroukhi[1], S. Pelloni[1], E. Bauge[2], and A. Koning[3]

[1] Paul Scherrer Institut, Villigen, Switzerland
[2] CEA, DAM, DIF, 91297 Arpajon cedex, France
[3] Nuclear Data Section, International Atomic Energy Agency, Vienna, Austria & Uppsala University, Uppsala, Sweden

Received: 27 February 2019 / Revised: 2 May 2019
Published online: 20 September 2019

Abstract. This paper presents an application of the Backward-Forward Monte Carlo (BFMC) method using measured critical boron concentrations for a specific PWR cycle. The considered prior nuclear data are the fission cross sections, $\overline{\nu}_p$ for ^{235}U and ^{239}Pu and the capture cross section of ^{238}U. The posterior nuclear data exhibit cross-isotope correlations, moderate changes for the average quantities and reduced uncertainties. This work is the first one considering the BFMC method and an integral system mostly sensitive to thermal neutrons. It contributes to show the impact of integral experimental data for the evaluation of nuclear data and their covariance matrices, leading to cross-isotope correlations and a nuclear data uncertainty reduction.

1 Introduction

Since a few years there is a growing reflection in the nuclear data community on the possible use of integral information directly at the evaluation level. Such integral information can include criticality benchmarks, reactor or shielding experiments and provides in a word ratios such as C/E, with C the calculated quantity from a simulated experiment with a measured value E. There are surely advantages to include integral information during the evaluation of nuclear data: improved nuclear data (*e.g.*, cross sections) leading to C/E closer to 1 and often reduced uncertainties ΔC, due to either a reduction of nuclear data uncertainties or new nuclear data correlations (or both). But there is also a certain level of risk: such evaluated nuclear data library might give better C/E values for specific calculations, but also degrade its performances for integral systems not included in the evaluation process. Up to now, there is no consensus at the evaluation level and the use of integral experiments is done on a case-by-case and *ad hoc* basis.

Independently of solving the above dilemma, the nuclear data literature already offers examples for the use of integral experiments. From a practical point of view, the fast-neutron criticality benchmarks and k_{eff} (neutron multiplication factor) offer a convenient playfield when combined with a tool, such as MCNP [1]. Such simulations can be performed in minutes on modern computers, with a high level of precision and the nuclear data libraries can easily be altered. It is therefore not surprising that the first demonstrations for the impact of using integral experiments concern systems such as Jezebel, Bigten or Godiva [2–7], leading to improved C/E, new (and adjusted) nuclear data and covariance matrices. One example considering a thermal benchmark for spent fuel storage can be found in ref. [8], but without specific feedback to nuclear data as its goal was towards spent nuclear fuel storage and not nuclear data evaluation. More recently, ref. [9] presents the results of the MOCABA model applied to PWR operation parameters, with feedback to nuclear data. The results presented in this reference are later compared with the present findings.

In practice however, the responses of simulations of selected integral experiments are already taken into account during the evaluation process of nuclear data, at least for major libraries such as JEFF-3.3 [10], ENDF/B-VIII.0 [11] or TENDL-2017 [12, 13]. Specific nuclear data such as $\overline{\nu}_p$ (average prompt neutron number emitted per fission) or fission cross sections for important actinides are partly modified to provide C/E of 1 for certain benchmarks, within the allowed degrees of freedom given by differential measurements and their uncertainties. But such *final* adjustments (or evaluation) do not come from a mathematical procedure as in the case of considering measured cross sections at a specific energy and for a specific isotope.

[a] e-mail: dimitri-alexandre.rochman@psi.ch

Different methods already exist for mathematically taking into account the feedback from integral simulations and have been demonstrated to provide better C/E values. The above examples (refs. [2–5]) are based on Bayesian Monte Carlo methods as presented in refs. [14–17], whereas refs. [8,9] combine Monte Carlo and Generalized Linear Least-Squares methods (GLLS). One can also cite the extensive studies within international groups using different variants of the GLLS methods [18], Unified Monte Carlo [19,20], the Petten method [21], variant of the GLLS method such as APIA [22], or Bayesian Monte Carlo methods combined with model defects [23,24]. The Bayesian Monte Carlo (BMC) and Backward-Forward Monte Carlo (BFMC) methods can be considered as practical solutions, allowing to avoid many usual approximations (Gaussian distributions and linearity) and can conveniently be included in the nuclear data evaluation process when combined with the Total Monte Carlo approach [25]. It was nevertheless recently shown that attention should be paid for the *curse of dimensionality*, which tends to limit the application of the classical BMC method [26] when using a large number of integral benchmarks. The required computer power associated with Monte Carlo method can also be a limiting factor.

In the example studied in the present paper, the BFMC method will be applied with a single source of integral information. Unlike the previous examples, a thermal system will be considered (critical boron letdown curve from a Pressurized Water Reactor (PWR)), leading to correlations between the relevant ^{235}U, ^{238}U and ^{239}Pu nuclear data, uncertainty reduction, and nuclear data posterior (in a Bayesian sense). Such results will be an additional element to be considered when trying to resolve the dilemma presented in the first part of the introduction: taking into account or not integral measurements in the thermal, resonance and fast neutron range can lead to different nuclear data; shall they be mathematically considered at the evaluation level?

The structure of this paper will closely follow the one of refs. [2,3] for an easier comparison. The method will be shortly presented (being the same as in these references), followed by the application to the critical boron letdown curve, and finally its impact on specific nuclear data.

2 Correlation from integral measurements

As mentioned before, the BFMC method was already extensively presented in a few papers, and readers are referred to refs. [2,3,15] for applications similar to this study. In the following, a minimal description is presented.

The BMC and BFMC methods are based on the availability of random nuclear data. Such quantities can come from varying parameters for models providing variations of nuclear data (as was done in the three references above), or from covariance information as included in nuclear data libraries. Examples of the use of such random nuclear data produced from covariance matrices are presented in refs. [27–30]; such method presents the advantage of Monte Carlo uncertainty propagation (repeating a large number of times the same simulation, each time changing the input nuclear data), based on a validated suite of simulation codes and nuclear data libraries. These codes do not necessary need to be stochastic. It is therefore very useful in reactor physics where the freedom of choice for simulation tools is relatively limited due to specific Quality Assurance procedures. As the reactor system selected in this work is following such stringent procedures, the random nuclear data are generated following the method described in refs. [27,31], using the covariance files from the ENDF/B-VII.1 library [32] (*i.e.* Cholesky decomposition of the covariance matrices, assuming Gaussian distributions for all nuclear data). The choice of this library for the covariance matrices allows consistency with the nominal nuclear data used in the simulation codes (see next paragraph).

Once the random nuclear data are available in the desired format (being similar to ref. [27]), each random set of nuclear data is used in a simulation to calculate a quantity for which J experimental data are available (called $B_{\mathrm{exp},\,j=1\ldots J}$ in the following). In the present case, the deterministic simulation tools are CASMO-5 for the lattice calculations [33] and SIMULATE-5 for the core calculations [34] (see ref. [27] for details) and the nuclear data covariance matrices are processed in 19 energy groups from 0 to 20 MeV (see table 1). If $i = (1 \ldots n)$ random nuclear data libraries are produced, calculations of $B^{(i)}_{\mathrm{calc},j}$ are repeated with each of the n libraries. A weight w_i for each set i can be calculated with the following equations:

$$\chi^2_i = \sum_{j=1}^{J} \left(\frac{B^{(i)}_{\mathrm{calc},j} - B_{\mathrm{exp},j}}{\Delta B_{\mathrm{exp},j}} \right)^2 , \tag{1}$$

$$w_i = \exp\left[- \left(\frac{\chi^2_i}{\chi^2_{\min}} \right)^2 \right] . \tag{2}$$

Note that the sum of the weights are not equal to 1. In the present case, the experimental uncertainties $\Delta B_{\mathrm{exp},j}$ are also needed and are detailed in sect. 3.1. The quantity $B^{(i)}_{\mathrm{calc},j}$ represents the calculated value based on the random nuclear data library i, and $\chi^2_{\min}$ is the minimum of all the χ^2_i. Such definition in eq. (1) is similar to a simplified χ^2, *i.e.* without taking into account experimental correlations between the different J measurements. The definition of eq. (2) is the main difference between BMC and BFMC. In the BMC approach, the exponential term is simply $-\chi^2_i/2$,

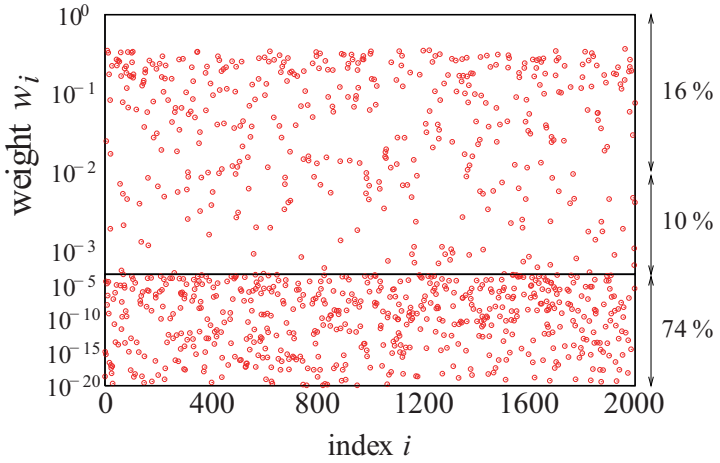

Fig. 1. Example of weights w_i calculated with eq. (2) in the present case. The varied nuclear data are ^{235}U(n, f), ^{235}U–$\overline{\nu}_p$, ^{238}U(n, γ), ^{239}Pu–$\overline{\nu}_p$ and ^{239}Pu(n, f). The experimental data are presented in sect. 3.1. The horizontal solid line indicates a break in the Y-axis with a zoom above $w_i > 10^{-5}$.

which supposes a proper estimation of χ^2_i from eq. (1), for instance using the definition of a general χ^2. The BFMC is a practical solution in the case eq. (1) cannot be estimated with the general χ^2 due to the lack of information (*e.g.* not enough experimental information). The definition of eq. (2) has a similar effect as using model defects, without a sound-mathematical approach [35].

To illustrate the weights obtained from eq. (2), fig. 1 presents the w_i values as obtained in this work (see next sections for details), following the representation of ref. [3]. Such distribution of weights indicates the quality of the random calculations with respect to the measured values. If a large proportion of weights are small compared to e^{-1} ($w_i = e^{-1} \simeq 0.37$ being the maximum value with $\chi^2_i = \chi^2_{\min}$), it indicates that the variation of nuclear data does not lead to a good agreement with the experimental data. Such issue is already discussed in ref. [26] and is quantified in the following with the equivalent sample size [36]. The approximation linked to the definition of χ^2_i is discussed at the end of the paper.

As presented in ref. [3], simple equations can be used to calculate weighted averages, weighted standard deviations and correlations between nuclear data, which will be used to represent the prior and posterior probability density functions and their associated covariances. They are repeated here for completeness. In the following, the nuclear data (cross sections or $\overline{\nu}_p$) will be represented by σ_α or σ_β, avoiding to indicate the variable for the incident neutron energy. Considering one type of nuclear data σ_α (for instance, the ^{235}U(n, f) at 10 eV), the prior average and variance from the n samples are

$$\overline{\sigma_\alpha}^{(\text{prior})} = \frac{1}{n}\sum_i^n \sigma_{\alpha,i} \tag{3}$$

$$\text{var}_\alpha^{(\text{prior})} = \frac{1}{n}\sum_i^n \left(\sigma_{\alpha,i} - \overline{\sigma_\alpha}^{(\text{prior})}\right)^2 . \tag{4}$$

As 19 energy groups are considered, the above equations are applied 19 times, one time for each energy group, leading to 19 averages and variances for one type of nuclear data (*e.g.*, the fission cross section of ^{235}U). For two types of nuclear data σ_α and σ_β, the covariance and correlation are defined as

$$\text{cov}_{\alpha\beta}^{(\text{prior})} = \frac{1}{n}\sum_i^n (\sigma_{\alpha,i} - \overline{\sigma_\alpha}^{(\text{prior})}) \cdot (\sigma_{\beta,i} - \overline{\sigma_\beta}^{(\text{prior})}) \tag{5}$$

$$\rho_{\alpha\beta}^{(\text{prior})} = \frac{\text{cov}_{\alpha\beta}^{(\text{prior})}}{\sqrt{\text{var}_\alpha^{(\text{prior})} \cdot \text{var}_\beta^{(\text{prior})}}} . \tag{6}$$

Again, 19×19 values are obtained for two specific nuclear data σ_α and σ_β when varying the incident neutron energy.

The standard errors *Std* on these quantities are defined as

$$Std\left(\overline{\sigma_\alpha}^{(\mathrm{prior})}\right) = \sqrt{\frac{\mathrm{var}_\alpha^{(\mathrm{prior})}}{n}}\,, \tag{7}$$

$$Std\left(\mathrm{var}_\alpha^{(\mathrm{prior})}\right) = \sqrt{\frac{2\,\mathrm{var}_\alpha^{(\mathrm{prior})}}{n-1}}\,, \tag{8}$$

$$Std\left(\rho_{\alpha\beta}^{(\mathrm{prior})}\right) = \sqrt{\frac{1-{\rho_{\alpha\beta}^{(\mathrm{prior})}}^2}{n-2}}\,. \tag{9}$$

In the case of posterior quantities being obtained with the use of the weights w_i, the previous equations for the moments and the correlation can be expressed in a similar way as

$$\omega = \sum_i^n w_i, \tag{10}$$

$$\overline{\sigma_\alpha}^{(\mathrm{post})} = \frac{1}{\omega}\sum_i^n w_i \cdot \sigma_{\alpha,i}, \tag{11}$$

$$\mathrm{var}_\alpha^{(\mathrm{post})} = \frac{1}{\omega}\sum_i^n (\sigma_{\alpha,i} - \overline{\sigma_\alpha}^{(\mathrm{post})})^2 \cdot w_i, \tag{12}$$

$$\mathrm{cov}_{\alpha\beta}^{(\mathrm{post})} = \frac{\sum_i^n (\sigma_{\alpha,i} - \overline{\sigma_\alpha}^{(\mathrm{post})}) \cdot (\sigma_{\beta,i} - \overline{\sigma_\beta}^{(\mathrm{post})}) \cdot w_i}{\omega}\,, \tag{13}$$

$$\rho_{\alpha\beta}^{(\mathrm{post})} = \frac{\mathrm{cov}_{\alpha\beta}^{(\mathrm{post})}}{\sqrt{\mathrm{var}_\alpha^{(\mathrm{post})} \cdot \mathrm{var}_\beta^{(\mathrm{post})}}}\,. \tag{14}$$

The standard errors of these quantities cannot be calculated simply based on the sample size n, but the so-called "equivalent sample size" [37], or ESS, defined as

$$ESS = \left(\sum_i^n w_i\right)^2 \Big/ \sum_i^n w_i^2, \tag{15}$$

needs to be used:

$$Std\left(\overline{\sigma_\alpha}^{(\mathrm{post})}\right) = \sqrt{\frac{\mathrm{var}_\alpha^{(\mathrm{post})}}{ESS}}\,, \tag{16}$$

$$Std\left(\mathrm{var}_{\sigma_\alpha}^{(\mathrm{post})}\right) = \sqrt{\frac{2\,\mathrm{var}_\alpha^{(\mathrm{post})}}{ESS-1}}\,, \tag{17}$$

$$Std\left(\rho_{\alpha\beta}^{(\mathrm{post})}\right) = \sqrt{\frac{1-{\rho_{\alpha\beta}^{(\mathrm{post})}}^2}{ESS-2}}\,. \tag{18}$$

The ESS quantity is a parameter indicating how the random calculations contribute to the posterior. A low ESS for large n would indicate that only a small number of random calculations is in good agreement with the measured values. In ref. [3] the ESS value was about 740 for $n = 7000$ ($\simeq 9\%$) (using a single criticality benchmark). In the present case, ESS is about 212 for $n = 2000$ ($\simeq$ 9–10%). In both cases, as indicated in fig. 1 for the present calculations, about 16% of the random nuclear data libraries are in good agreement with the measurements. It is notably different in ref. [26] where the ESS sharply falls with the use of multiple benchmarks. Note that large ESS values do not assure that all "importance regions" have been sampled.

Finally, as an indication of the convergence for calculated averages, standard deviations and correlations between nuclear data, fig. 2 presents these quantities for two representative examples ($^{238}\mathrm{U}(\mathrm{n},\gamma)$ cross section at 149 eV and $\overline{\nu}_p$ of ^{235}U at 0.35 eV). The shadow bands represent the standard errors for the prior and posterior quantities.

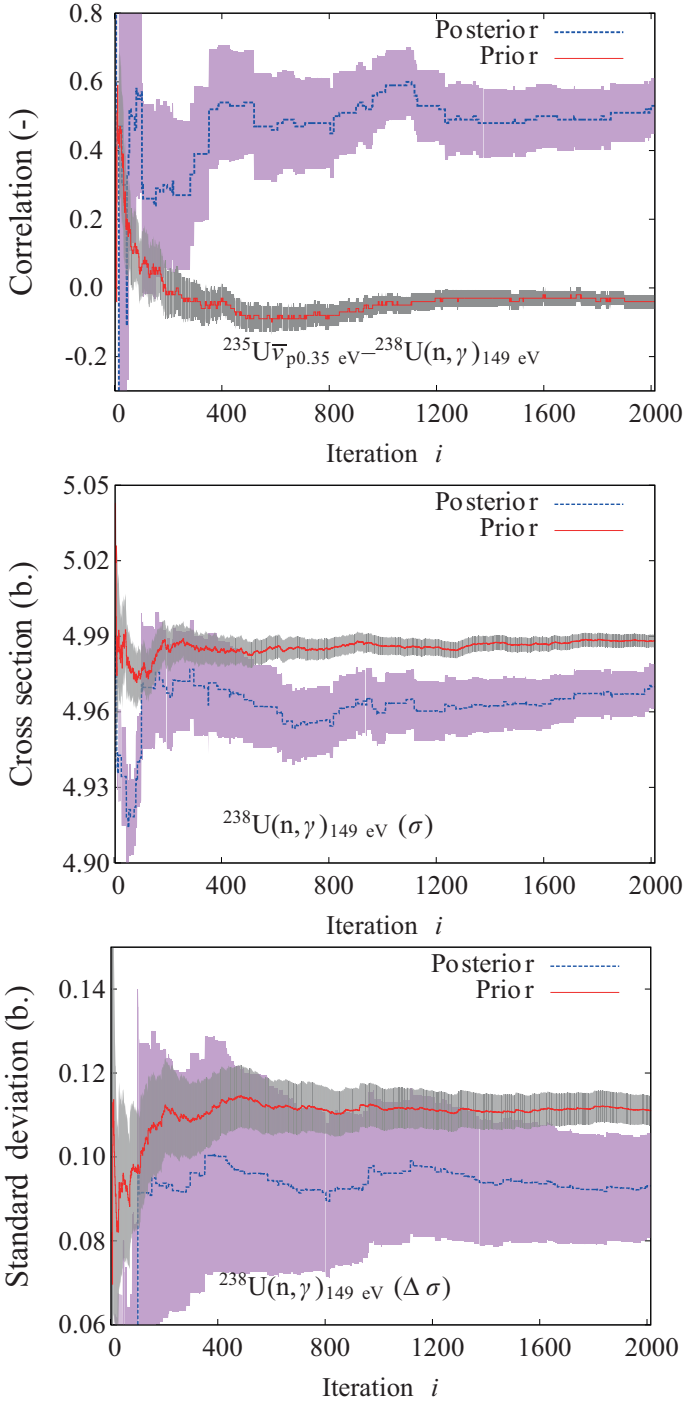

Fig. 2. Example of the running correlation ρ between the $\overline{\nu}_p$ of ^{235}U at 0.35 eV and the ^{238}U(n, γ) cross section at 149 eV (top), and mean (middle) and standard deviation (bottom) for the ^{238}U(n, γ) cross section at 149 eV.

3 Application to ^{235,238}U and ^{239}Pu

The work presented in refs. [2, 3, 26] was dedicated to the fast neutron range, using criticality benchmarks. In order to obtain nuclear data correlations due to a system mostly sensitive to thermal neutrons, the case of a Swiss PWR is selected, with a specific core loading pattern corresponding to a single cycle (representing approximately one year of irradiation). In the following, five specific nuclear data types are considered: ^{235}U–$\overline{\nu}$, ^{235}U(n, f), ^{238}U(n, γ), ^{239}Pu–$\overline{\nu}$ and ^{239}Pu(n, f), as they are the main contributors to the observable uncertainty (see next section). A total of $5\times19 = 95$ nuclear data sets are thus analyzed: 5 reactions with 19 energy groups. The energy grid is presented in table 1.

Table 1. Energy grid for the 19 groups used in this study.

Group	1	2	3
Boundary	20–5 MeV	5–1 MeV	1–0.019 MeV
4	5	6	7
19–5.5 keV	5.5–0.15 keV	150–48 eV	48–28 eV
8	9	10	11
28–16 eV	16–6.8 eV	6.8–6.5 eV	6.5–4 eV
12	13	14	15
4–2 eV	2–0.625 eV	625–350 meV	350–300 meV
16	17	18	19
0.3–0.19 eV	190–100 meV	100–30 meV	30–0.01 meV

Table 2. Impact in percent of the variations of specific nuclear data at the middle of cycle (close to 150 efpd). The 5 reactions are $^{235}U_{\overline{\nu}_p}$, $^{235}U(n,f)$, $^{238}U(n,\gamma)$, $^{239}Pu(n,f)$ and $^{239}Pu_{\overline{\nu}_p}$.

Data	All	light	minor actinides	5 reactions considered here
Impact (%)	12	1.2	1.9	11

The simulation of the reactor cycle is performed as follows. First the lattice code CASMO-5 is used to generate macroscopic cross sections for each assembly type of the core. Such macroscopic cross section tables are produced for different conditions of the core, considering for instance different coolant and fuel temperatures, core pressure, assembly burnup values. Nuclear data (*processed microcospic cross sections*) are used in CASMO-5 for the generation of such tables. The energy grid of the nuclear data is 586 groups. The random variations from the ENDF/B-VII.1 covariance matrices are applied at the CASMO-5 level, on the 19 energy-group structure [27]. This way, random macroscopic cross sections for each assembly type are generated. The second step consists in simulating the core cycle with SIMULATE-5, based on the generated random macroscopic cross sections from CASMO-5 (one calculation i is based on one random set of microcospic cross sections). SIMULATE-5 simulates many quantities during the core burnup, such as the assembly/pin burnup, fuel composition, reactivity, temperature, pressure, and also boron concentration, later compared with measured values. Such calculations are performed at specific time or core burn-up steps, depending on the variations of the core conditions. In the present case, a total of 12 steps are considered from the beginning of cycle (BOC) to the end of cycle (EOC). More details can be found in ref. [38] as the calculation scheme used in this work is similar with one noticeable difference being the origin of the covariance matrices.

3.1 Boron letdown curve from a PWR cycle

As mentioned, a specific cycle for the PWR of interest is selected for this study. The observables (measured quantities) are the amounts of soluble boron as a function of the cycle time (also called "efpd" for effective full power day). Such measurements correspond to the amount of soluble boron used during the PWR cycle so that the reactor core stays at a critical level ($k_{\text{eff}} = 1$): at the start of a reactor cycle (BOC), the excessive amount of reactivity due to the fresh fuel is compensated by adding soluble boron in the primary coolant. As the core is being burnt as a function of time, the excess reactivity decreases and less boron is added. These amounts of boron are regularly measured and can be compared with calculated values when simulating the reactor cycle with a tool such as SIMULATE. The comparison between measured and calculated boron concentration is usually part of the validation of the PWR calculation scheme, as presented in ref. [38]. The measured boron concentration is presented in fig. 3, together with the prior and posterior letdown curves. The uncertainties ΔB_{exp} considered here are about 30 ppm (it has been reported in refs. [39,40] that the measured uncertainties can be as low as 20 ppm). In the present case, the core calculations are performed at 12 state points, and the calculated boron concentration are measured with $J = 12$ experimental values.

As mentioned, the variations in the calculated boron concentrations are due to the random nuclear data used for each individual simulation. Based on the ENDF/B-VII.1 covariance matrices, different nuclear data were simultaneously varied: all (as included in ENDF/B-VII.1, sampled 1000 times), only light isotopes (up to ^{16}O, sampled a few hundred of times), only the minor actinides (also sampled a few hundreds of times) and finally only 5 quantities: $^{235}U_{\overline{\nu}_p}$, $^{235}U(n,f)$, $^{238}U(n,\gamma)$, $^{239}Pu(n,f)$ and $^{239}Pu_{\overline{\nu}_p}$ (sampled 2000 times). The impact of such variations on the boron concentration at the middle of cycle (MOC) are presented in table 2. The main contributors to the total uncertainties are the five nuclear data quantities mentioned above, with a total uncertainty of 11% on the boron concentration.

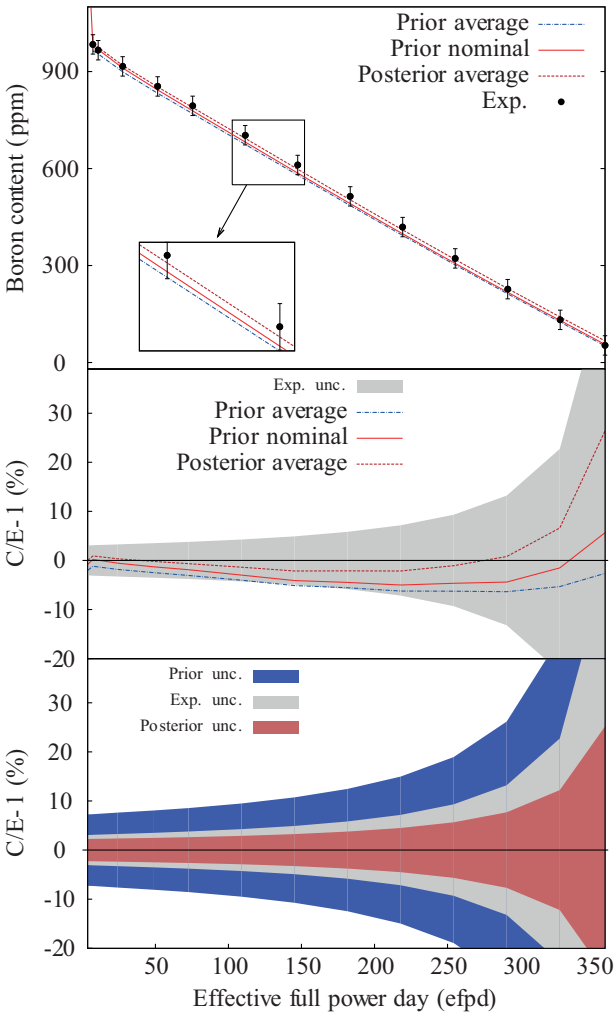

Fig. 3. Top: Example of the calculated and measured boron concentrations as a function of cycle length (irradiation time). The "nominal" curve represents the calculation with unperturbed nuclear data, and the "average" represents the average over the n random cases. Middle: Ratio C/E-1 in percent for the different calculated curves. Bottom: experimental and calculated uncertainties on the boron concentration.

In refs. [7,41], it was also observed that ^{235,238}U and ^{239}Pu are the main contributors to the uncertainty on the boron concentration, and the total calculated uncertainties vary from 7 to 15% (using different simulation tools and nuclear data libraries). The effect of light isotopes such as ^{1}H, ^{16}O or ^{10,11}B do not have a significant impact on the calculated boron concentration.

Due to the quality of the validated models, simulation codes and nuclear data, the agreement between the prior nominal calculation and measurements is already relatively good (see fig. 3), with a simplified reduced χ^2_{nominal} of 0.26. For the prior average calculations, the simplified reduced $\chi^2_{\text{prior average}}$ is equal to 0.56. Note that the prior calculated uncertainties are larger than the measured ones. The posterior average calculated boron concentrations ($\chi^2 = 0.08$) will therefore not reflect any possible prior biases due to the simulation scheme. There is a certain similarity with the work from refs. [2,3,26] as the calculated uncertainties were also larger than the measured ones; but in this work, the nominal calculation (without nuclear data variations) is already in good agreement with the measured value. In the next sections, the posterior nuclear data will be presented.

3.2 Nuclear data correlations

It is expected that the use of the boron concentration to calculate the weights w_i will modify the nuclear data, in terms of average values, uncertainties, and also correlations. This was demonstrated in the mentioned references for systems sensitive to fast neutrons, and the same is anticipated here. One main argument is that the calculated prior uncertainties are larger than the measured ones (see fig. 3): therefore the posterior nuclear data uncertainties will

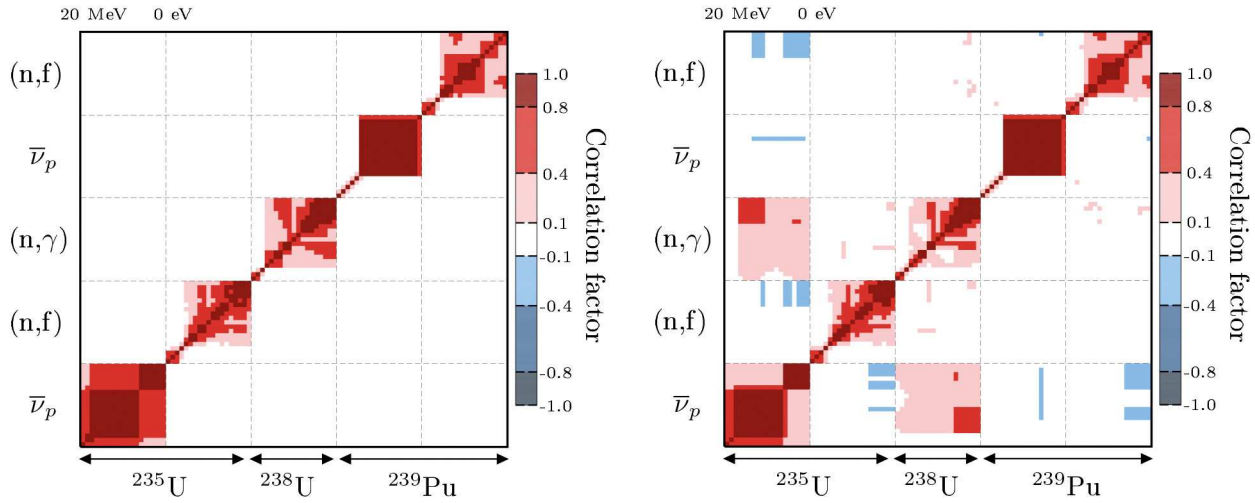

Fig. 4. Correlation matrices between the three different isotopes for the prior (top) and posterior (bottom) calculations, considering the measured critical boron concentrations during the PWR cycle. In each sub-box, the neutron energy is decreasing from 20 MeV to 0 eV from left to right.

be smaller than the prior ones, and (or) additional correlations between the nuclear data will appear. Prior and posterior nuclear data correlations are presented in fig. 4, using the measured critical boron concentrations. The prior correlation matrix is similar to the one given in the ENDF/B-VII.1 library (reconstructed from the Monte Carlo variations of the considered nuclear data), and also representative of the other libraries: a certain degree of energy-energy correlation exists for specific reactions (such as ^{238}U(n, γ)-^{238}U(n, γ)), but due to the evaluation methods, there are no prior correlations between $\overline{\nu}_p$ and fission cross sections. Also, no prior correlations are given between isotopes. It was shown in refs. [2,3] that cross correlations between isotopes can be obtained when using integral data, but also using differential measurements such as measurements on natural targets [42].

The posterior correlation matrix is indicating non-zero correlations between isotopes, especially between ^{235}U-$\overline{\nu}_p$ and ^{238}U(n, γ). This can be expected: as the measured boron concentration is proportional to the reactor criticality level, an excess in neutron can be compensated by an increase in their disappearance (such as via capture reaction). Similar reasoning can be applied for the anti-correlations. This effect of compensation between neutron production and disappearance is similar to the one observed in ref. [3] with the imf7 (Bigten) benchmark.

3.3 Posterior cross sections and variances

In the present case, as the prior nuclear data distributions are assumed to be Gaussian, and as the associated standard deviations are relatively small for the reactions of interest, the posterior distributions are also Gaussian with skewness values close to zero. Additionally to the posterior correlations, one can calculate the posterior nuclear data and their standard deviations, as presented in fig. 5 in terms of ratios between the posterior and prior quantities. The changes generated by the BFMC update are driven by the prior agreement between the experimental data and the calculated boron concentration. The prior average boron concentration is slightly smaller than the measured one (*e.g.*, in fig. 3 at 150 efpd, the calculated average prior concentration is 580 ± 63 ppm, whereas the average posterior concentration is 607 ± 20 ppm; the measured value being 611 ± 30 ppm). There is therefore a need to increase the reactivity and to decrease the uncertainties to obtain a better agreement between calculated and measured values.

The average nuclear data are not strongly changed (less than 1%), as the prior calculations were already in good agreement with the measurements. The major impact is on the ^{238}U(n, γ) cross section between 4 eV and 5 keV. In this energy range, the neutron absorption by ^{238}U is important. The decrease of this cross section therefore contributes to the increase of reactivity.

As for the standard deviations, the prior and posterior uncertainty of the boron concentration are presented in fig. 3, bottom. Such decrease is due to the uncertainty reduction for $\overline{\nu}_p$ for ^{235}U and ^{238}U(n, γ).

In ref. [9], posterior cross sections are also presented, based on updates from boron concentrations. This study is very similar to the present one, still presenting some differences, making difficult a direct comparison. If the considered covariance files are similar (from ENDF/B-VII.1), the reference libraries are different (ENDF/B-VII.1 in the present case, and the WIMS reference library in [9]). One noticeable difference concerns the prior agreement between the calculated and measured boron concentrations: whereas the calculations are within the experimental uncertainties

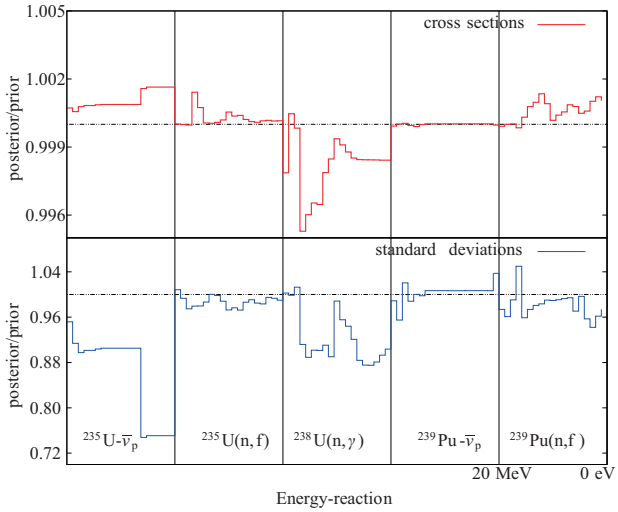

Fig. 5. Top: Ratios of posterior over prior nuclear data (cross sections and $\overline{\nu}_p$). Bottom: same for standard deviations. The five vertical segments represent the five considered reactions, with decreasing energy from the left to the right for each segment.

Table 3. Comparisons between the prior and the posterior data at thermal energy (in barns for the cross sections). The column "Standard" refers to the standard cross sections and $\overline{\nu}_p$ from ref. [43].

Reaction	Standard	Prior	Posterior
^{235}U(n, f)	587.3 ± 1.4	585.1 ± 2.3	585.2 ± 2.3
^{238}U(n, γ)	2.678 ± 0.016	2.694 ± 0.050	2.690 ± 0.045
^{239}Pu(n, f)	752.4 ± 2.2	751.3 ± 8.4	752.1 ± 8.2
^{235}U-$\overline{\nu}_p$	2.425 ± 0.011	2.437 ± 0.018	2.441 ± 0.013
^{239}Pu-$\overline{\nu}_p$	2.878 ± 0.013	2.879 ± 0.005	2.879 ± 0.005

in the present case, they are lower in ref. [9]. Also, the simulation tool is different, as well as the updating method (MOCABA *vs.* BFMC). In conclusion, the proposed variations are different compared to the present results: three cross sections (^{239}Pu(n, f), ^{235}U(n, f) and ^{238}U(n, γ)) are considered in ref. [9], the other ones were showing low impact. If the observed trends are similar for ^{239}Pu(n, f), they are opposite for the uranium isotopes. Additionally, the nubar of ^{235}U is showing here a non-negligible impact. Without a detailed analysis of these differences, one can certainly conclude that the nuclear data updates are sensitive to the considered simulation systems, nuclear data libraries and measurements. This last point is discussed in the last section "Discussion".

The posterior values presented in fig. 5 can be compared with current nuclear data evaluations such as from the "neutron data standard" [43]. Table 3 presents the standard values with the ENDF/B-VII.1 prior and posterior data (in barns for the cross sections). As observed in fig. 5, the posterior and prior data (at thermal energy) are very close. Additionally, all the thermal posterior data from table 3 are in agreement with the standard evaluations. Such agreement can be obtained because the prior (ENDF/B-VII.1) and the standard values are already consistent. It would be interesting to observe similar results if repeating this study with a prior library different from ENDF/B-VII.1, and different from ref. [43].

3.4 Resulting boron concentration distributions

The posterior boron concentration presents a better agreement with the measurements, both for the average values as well as for the uncertainties. As indicated, the value for the concentration at 150 efpd is much closer to the measured quantity. The posterior uncertainty is smaller than the measured one, certainly because there is a common effect of considering 12 independent measured points together. Such prior and posterior distributions for MOC and EOC are presented in fig. 6. The distribution at 150 efpd is representative for the other irradiation times, even if the bias between measured and calculated values is slightly changing as a function of time (see fig. 3).

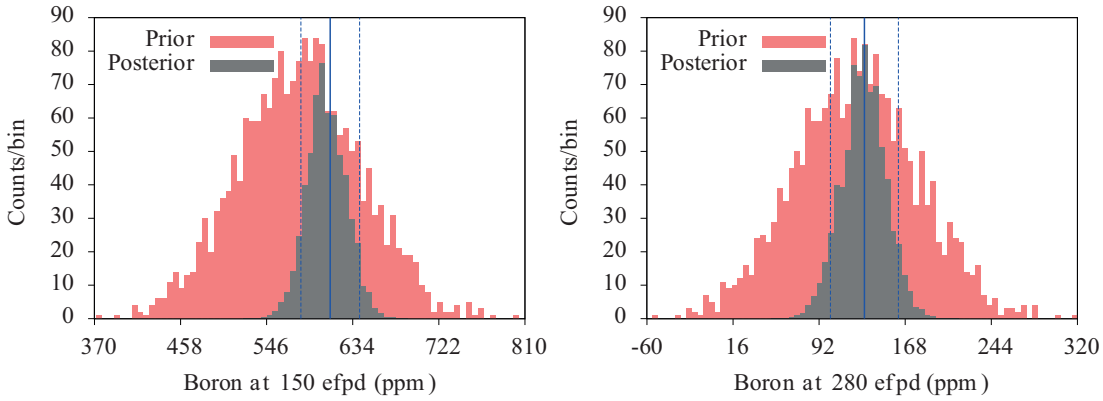

Fig. 6. Prior and posterior distributions for the boron concentrations at 150 efpd (middle of cycle) and 280 efpd (end of cycle). The solid vertical line indicates the measured value and the dashed lines represent the experimental uncertainties.

4 Discussion

This work is an additional illustration of the advantages of taking into account integral data when evaluating nuclear data, their uncertainties and correlations. If this is certainly not new, this study clearly indicates the reduction of uncertainties on the considered reactor measurements, and the implications this has on specific nuclear data and their probability density functions. As commented before, previous studies using the Bayesian Monte Carlo method or one of its variations also point out to the same conclusions, but for systems mostly sensitive to fast neutrons. The originality here is that the posterior nuclear data are obtained for a thermal system with the BFMC method.

Still, the possible drawbacks of such adjustments are not explored. In a complete nuclear data evaluation work, the impact of the changes presented in fig. 5 needs to be assessed by considering other integral systems. Given a large-enough database of trusted integral data, it will be possible to build some confidence in the adjusted nuclear data. This is not the case in the work presented here, where only one thermal system is considered. It would be judicious to combine the observed changes with the ones for instance coming from thermal criticality benchmarks or with the system studied in ref. [9]. As part of the exploratory work, two thermal criticality benchmarks were used with the updated ^{235}U and ^{238}U cross sections: leu-comp-therm-003.1 and leu-comp-therm-005.1. The posterior cross sections lead to an increase in k_{eff} of 250 to 300 pcm, resulting from the decrease of the capture cross section of ^{238}U. This indicates that in a work combining these two benchmarks with the system presented in this work, the changes in cross sections would be less likely.

It is also important to realize that the nuclear data considered in this work for adjustment do not cover all types. The sampling is performed based on the available covariance information from the ENDF/B-VII.1 library and does not include angular distributions or thermal scattering data. This undeniably leads to adjustments dedicated to the studied system (library, processing, code and applications).

A few comments relevant to the original question presented in the introduction can be proposed (*Shall the integral information be mathematically included in the evaluation process?*). The discussion related to this question invokes the fact that the use of integral experiments modifies the nuclear data and their covariances and renders them less multi-purpose.

It is true that the covariance information depends on the method applied to evaluate them, as illustrated here. They will be different if integral information is included or not. When comparing the posterior correlations from fig. 4 with the ones from ref. [3] (*e.g.*, figs. 5 and 7) or from ref. [26] (fig. 10), it is visible that different integral experiments lead to different correlation matrices. There is nevertheless no conceptual difference when using differential data (*e.g.*, pointwise cross sections): a cross section derived from a time-of-flight measurement (for instance at the GELINA, nTOF, or RPI facilities) will be accompanied with a different energy-energy correlation matrix from the same cross section measured with a Lead-Slowing down spectrometer. Additionally, as the nuclear data evaluation process makes use of reaction models, the energy-energy correlation matrix will also be different, for instance depending on the choice of the optical model. On that account, the use of integral information during the nuclear data evaluation process cannot be rejected.

The second argument indicating that the posterior (average) nuclear data, not the covariance matrices, will be of less general use when obtained from both differential and integral information needs to be studied more in detail and cannot easily be answered. One needs to keep in mind that for the time being, a number of general-purpose libraries is solely validated with a small number of benchmarks, mostly related to criticality during the evaluation process (other validations are performed after the library release and are not part of the evaluation process). The generality of these libraries is consequently already limited. It is therefore not obvious that using a selection of integral benchmarks (during the evaluation process) will make them even less general. However, as noticed in the previous paragraph with

the use of criticality benchmarks, it is of prime importance to proceed with integral adjustment considering various sources of information, if possible varying the simulation tools and the processing steps of the basic nuclear data. But such discussion goes beyond the work presented in this paper and is certainly not settled with this study. It will nevertheless be useful to consider different additional analysis on this matter.

As a final point, the definition of eqs. (1) and (2) has also an influence on the posterior distributions. If it is possible to carefully analyze all experimental points and derive a complete experimental covariance matrix, then the BMC method can be applied. In the present work, not enough information is known on the experimental data and their covariances, as it is unfortunately often the case. Under these limitations, the BFMC method offers a temporary convenient solution. As mentioned, a better solution lies in the recent work using model defects, and these possibilities will be soon explored for full nuclear data evaluations. For the time being, simplified methods such as BFMC provide an advantageous solution.

5 Conclusion

In this work, specific nuclear data and their covariance matrices were updated using the backward-forward Monte Carlo method and the measured boron concentrations for a specific PWR cycle. It was shown that the prior agreement between calculated and measured values was rather good, whereas the calculated uncertainties were larger than the ones from the measurements. The posterior nuclear data were mostly affected via their covariance matrices, presenting cross-isotope correlations which were not present in the prior estimation. From the nuclear data evaluation point of view, this study enters into the more-general discussion on the use (or not) of integral data during the evaluation process. Without giving a final answer, it points to a decrease of nuclear data uncertainties together with the rise of cross-isotope correlations.

This work was partly funded by the Swiss Nuclear Safety Inspectorate ENSI (H-101230) and was conducted within the framework of the STARS program (`http://www.psi.ch/stars`).

References

1. T. Goorley, *MCNP 6.1.1 - Beta release Notes*, Los Alamos National Laboratory, Report LA-UR-14-24680 (June 2014).
2. D. Rochman, E. Bauge, A. Vasiliev, H. Ferroukhi, Eur. Phys. J. N **3**, 14 (2017).
3. D. Rochman, E. Bauge, A. Vasiliev, H. Ferroukhi, G. Perret, Eur. Phys. J. N **4**, 7 (2018).
4. C. De Saint Jean, P. Archier, E. Privas, G. Noguere, B. Habert, P. Tamagno, Nucl. Data Sheets **148**, 338 (2018).
5. D. Siefman, M. Hursin, D. Rochman, S. Pelloni, A. Pautz, Eur. Phys. J. Plus **133**, 429 (2018).
6. T. Kawano, K.M. Hanson, S. Frankle, P. Talou, M.B. Chadwick, R.C. Little, Nucl. Sci. Eng. **153**, 1 (2006).
7. O. Cabellos, L. Fiorito, EPJ Web of Conferences **211**, 07008 (2019).
8. A. Hoefer, O. Buss, M. Hennebach, M. Schmid, D. Porsch, Ann. Nucl. Energy **77**, 514 (2015).
9. E. Castro, C. Ahnert, O. Buss, N. Garcia-Herranz, A. Hoefer, D. Porsch, Ann. Nucl. Energy **85**, 148 (2016).
10. *JEFF-3.3, Joint Evaluated Fission and Fusion File*, OECD/NEA, `https://www.oecd-nea.org/dbdata/jeff/jeff33/index.html`.
11. D.A. Brown *et al.*, Nucl. Data Sheets **148**, 1 (2018).
12. A.J. Koning, D. Rochman, Nucl. Data Sheets **113**, 2841 (2012).
13. A. Koning, D. Rochman J. Sublet, N. Dzysiuk, M. Fleming, S. van der Marck, Nucl. Data Sheets **155**, 1 (2019).
14. A.J. Koning, Eur. Phys. J. A **51**, 184 (2015).
15. E. Bauge, P. Dossantos-Uzarralde, J. Kor. Phys. Soc. **59**, 1218 (2011).
16. E. Bauge, M. Dupuis, S. Hilaire, S. Péru, A.J. Koning, D. Rochman, S. Goriely, Nucl. Data Sheets **118**, 32 (2014).
17. P. Helgesson, H. Sjostrand, D. Rochman, Nucl. Data Sheets **145**, 1 (2017).
18. M. Salvatores *et al.*, Nucl. Data Sheets **118**, 38 (2014).
19. R. Capote, D.L. Smith, Nucl. Data Sheets **109**, 2725 (2008).
20. R. Capote, D. Smith, A. Trkov, M. Meghzifene, J. ASTM Int. `https://doi.org/10.1520/JAI104115` (2012).
21. D. Rochman, A.J. Koning, Nucl. Sci. Eng. **172**, 287 (2012).
22. S. Pelloni, D. Rochman, Ann. Nucl. Energy **115**, 323 (2018).
23. P. Helgesson, H. Sjostrand, Rev. Sci. Instrum. **88**, 115114 (2017).
24. G. Schnabel, H. Leeb, EPJ Web of Conferences **111**, 09001 (2016).
25. A.J. Koning, D. Rochman, Ann. Nucl. Energy **35**, 2024 (2008).
26. D. Rochman, E. Bauge, A. Vasiliev, H. Ferroukhi, S. Pelloni, A.J. Koning, J.Ch. Sublet, Eur. Phys. J. Plus **133**, 537 (2018).

27. D. Rochman, A. Vasiliev, H. Ferroukhi, H. Dokhane, A. Koning, Ann. Nucl. Energy **112**, 236 (2018).
28. M. Klein, L. Gallner, B. Krzykacz-Hausmann, I. Pasichnyk, A. Pautz, W. Zwermann, *Influence of nuclear data covariance on reactor core calculations*, in *Proceedings of the International Conference on Mathematics and Computational Methods Applied to Nuclear Science and Engineering (M& C 2011) Rio de Janeiro, RJ, Brazil, May 8-12, 2011*, on CD-ROM.
29. C.J. Diez, O. Buss, A. Hoefer, D. Porsc, O. Cabellos, Ann. Nucl. Energy **77**, 101 (2015).
30. E. Castro, C. Ahnert, O. Buss, N. Garcia-Herranz, A. Hoefe, D. Porsch, Ann. Nucl. Energy **95**, 148 (2016).
31. A. Aures, F. Bostelmann, M. Hursin, O. Leray, Ann. Nucl. Energy **94**, 269 (2017).
32. M.B. Chadwick *et al.*, Nucl. Data Sheets **112**, 2887 (2011).
33. J. Rhodes, K. Smith, D. Lee, *CASMO-5 development and applications*, in *Proceedings of the PHYSOR-2006 conference, ANS Topical Meeting on Reactor Physics, Vancouver, BC, Canada, September 10-14, 2006* (ANS, 2006) p. B144.
34. T. Bahadir, S. Lindahl, *Studsvik's next generation nodal code SIMULATE-5*, in *Proceedings of the ANFM-2009 conference, Advances in Nuclear Fuel Management IV, Hilton Head Island, South Carolina, USA, April 12-15, 2009.*
35. G. Schnabel, *Large Scale Bayesian Nuclear Data Evaluation with Consistent Model Defects*, PhD thesis, TU Vienna, Austria, June 2015.
36. M.B. Priestley, *Spectral Analysis and Time Series 1* (Academix Press, 1982).
37. L. Kish, *Survey Sampling* (Wiley & Sons, Inc., NY, London, 1965).
38. O. Leray, H. Ferroukhi, M. Hursin, A. Vasiliev, D. Rochman, Ann. Nucl. Energy **110**, 547 (2017).
39. C. Demaziere, I. Pazsit, Nucl. Technol. **140**, 147 (2002).
40. A. Hoefer, O. Buss, *Application of Bayesian Monte Carlo Analysis to Criticality Safety Assessment*, in *ANS Winter Meeting, Washington, D.C., October 29–November 2* (2017).
41. O. Cabellos, W. Castro, C. Ahnert, C. Holgado, Nucl. Eng. Technol. **46**, 299 (2014).
42. J.-Ch. Sublet *et al.*, Eur. Phys. J. Plus **134**, 350 (2019).
43. A.D. Carlson, V.G. Pronyaev, R. Capote, G.M. Hale, Z.-P. Chen, I. Duran, F.-J. Hambsch, S. Kunieda, W. Mannhart, B. Marcinkevicius, R.O. Nelson, D. Neudecker, G. Noguere, M. Paris, S.P. Simakov, P. Schillebeeckx, D.L. Smith, X. Tao, A. Trkov, A. Wallner, W. Wang, Nucl. Data Sheets **148**, 143 (2018).